Supporting Information

Light-driven Hydrogen Evolution from Water by a Tripodal Silane Based $Co^{II}_6L^1_8$ Octahedral Cage

Mahesh S. Deshmukh,[a‡] Vishwanath S. Mane,[b‡] Avinash S. Kumbhar,[b]* and Ramamoorthy Boomishankar[a,c]*

[a]Department of Chemistry, Indian Institute of Science Education and Research, Pune-411008, India
[b]Department of Chemistry, Savitribai Phule Pune University, Pune-411007, India
[c]Centre for Energy Science, Indian Institute of Science Education and Research, Pune-411008, India
*Email: boomi@iiserpune.ac.in, askum@chem.unipune.ac.in

Table S1: Crystal data of cage **1**

Compound	**1**
Chemical formula	$C_{128}H_{134}Cl_{12}N_{24}O_6Si_8Co_6$
Formula weight	3106.21
Temperature	100(2)K
Crystal system	Orthorhombic
Space group	Pbcn
a (Å); α (°)	21.048(5); 90°.
b (Å); β(°)	29.141(7); 90 °.
c (Å); γ (°)	32.738(8); 90°.
V (Å^3); Z	20080(8); 150
ρ (calc.) mg m^{-3}	1.023
μ(Mo K$_\alpha$) mm^{-1}	0.735
2θ$_{max}$ (°)	50.052
R(int)	0.2118
Completeness to θ	99.9 %
Data / param.	17730/863
GOF	1.058
R1 [F>4σ(F)]	0.0768
wR2 (all data)	0.2642
max. peak/hole (e.Å^{-3})	1.105/-1.171

Table S2: Selected bond-lengths and angles for **1**.

Compound	**Bond length**		**Bond angle**	
1	Co(1)-O(1)	2.116(5)	O(1)-Co(1)-N(113)	87.4(2)
	Co(1)-N(113)	2.126(6)	O(1)-Co(1)-N(313)	87.8(2)
	Co(1)-N(313)	2.141(6)	N(113)-Co(1)-N(313)	175.1(2)
	Co(1)-N(213)	2.173(6)	O(1)-Co(1)-N(213)	89.0(2)
	Co(1)-N(433)#1	2.177(6)	N(313)-Co(1)-N(213)	89.9(2)
	Co(1)-Cl(1)	2.351(3)	O(1)-Co(1)-N(433)#1	90.0(2)
	Co(2)-O(2)	2.143(7)	N(113)-Co(1)-N(433)#1	89.8(2)
	Co(2)-N(123)	2.170(6)	N(313)-Co(1)-N(433)#1	91.2(2)
	Co(2)-N(123)#1	2.170(6)	N(213)-Co(1)-N(433)#1	178.5(2)
	Co(2)-N(223)#1	2.177(6)	O(1)-Co(1)-Cl(1)	179.30(16)
	Co(2)-N(223)	2.178(6)	N(113)-Co(1)-Cl(1)	92.59(18)
	Co(2)-Cl(2)	2.340(4)	N(313)-Co(1)-Cl(1)	92.18(17)
	Co(3)-O(3)	2.128(5)	N(213)-Co(1)-Cl(1)	90.32(16)
	Co(3)-N(233)	2.154(6)	N(433)#1-Co(1)-Cl(1)	90.69(16)
	Co(3)-N(413)	2.160(6)	O(2)-Co(2)-N(123)	87.91(15)

	Co(3)-N(333)	2.190(6)	N(123)-Co(2)-N(123)#1	175.8(3)
	Co(3)-N(133)#1	2.195(6)	O(2)-Co(2)-N(223)#1	90.71(15)
	Co(3)-Cl(3)	2.345(3)	N(123)-Co(2)-N(223)#1	90.5(2)
	Co(4)-O(4)	2.146(7)	N(123)#1-Co(2)-N(223)#1	89.6(2)
	Co(4)-N(423)	2.147(5)	O(2)-Co(2)-N(223)	90.71(15)
	Co(4)-N(423)#1	2.147(5)	N(123)-Co(2)-N(223)	89.6(2)
	Co(4)-N(323)	2.182(6)	N(123)#1-Co(2)-N(223)	90.5(2)
	Co(4)-N(323)#1	2.182(6)	N(223)#1-Co(2)-N(223)	178.6(3)
	Co(4)-Cl(4)	2.367(3)	O(2)-Co(2)-Cl(2)	180.0
			N(123)-Co(2)-Cl(2)	92.09(15)
			N(223)-Co(2)-Cl(2)	89.29(15)
			O(3)-Co(3)-N(233)	87.8(2)
			O(3)-Co(3)-N(413)	88.4(2)
			N(233)-Co(3)-N(413)	175.6(2)
			O(3)-Co(3)-N(333)	91.8(2)
			N(233)-Co(3)-N(333)	89.4(2)
			N(413)-Co(3)-N(333)	88.5(2)
			O(3)-Co(3)-N(133)#1	87.2(2)
			N(233)-Co(3)-N(133)#1	90.8(2)
			N(413)-Co(3)-N(133)#1	91.3(2)
			N(333)-Co(3)-N(133)#1	178.9(2)
			O(3)-Co(3)-Cl(3)	177.38(17)
			N(233)-Co(3)-Cl(3)	91.99(16)
			N(413)-Co(3)-Cl(3)	91.86(16)
			N(333)-Co(3)-Cl(3)	90.83(16)
			N(133)#1-Co(3)-Cl(3)	90.21(16)
			O(4)-Co(4)-N(423)	88.63(15)
			O(4)-Co(4)-N(423)#1	88.62(15)
			N(423)-Co(4)-N(423)#1	177.3(3)
			O(4)-Co(4)-N(323)	90.23(14)
			N(423)-Co(4)-N(323)	89.5(2)
			N(423)#1-Co(4)-N(323)	90.5(2)
			O(4)-Co(4)-N(323)#1	90.23(14)
			N(323)-Co(4)-N(323)#1	179.5(3)
			O(4)-Co(4)-Cl(4)	180.0
			N(423)-Co(4)-Cl(4)	91.37(15)
			N(423)#1-Co(4)-Cl(4)	91.38(15)
			N(323)-Co(4)-Cl(4)	89.77(14)

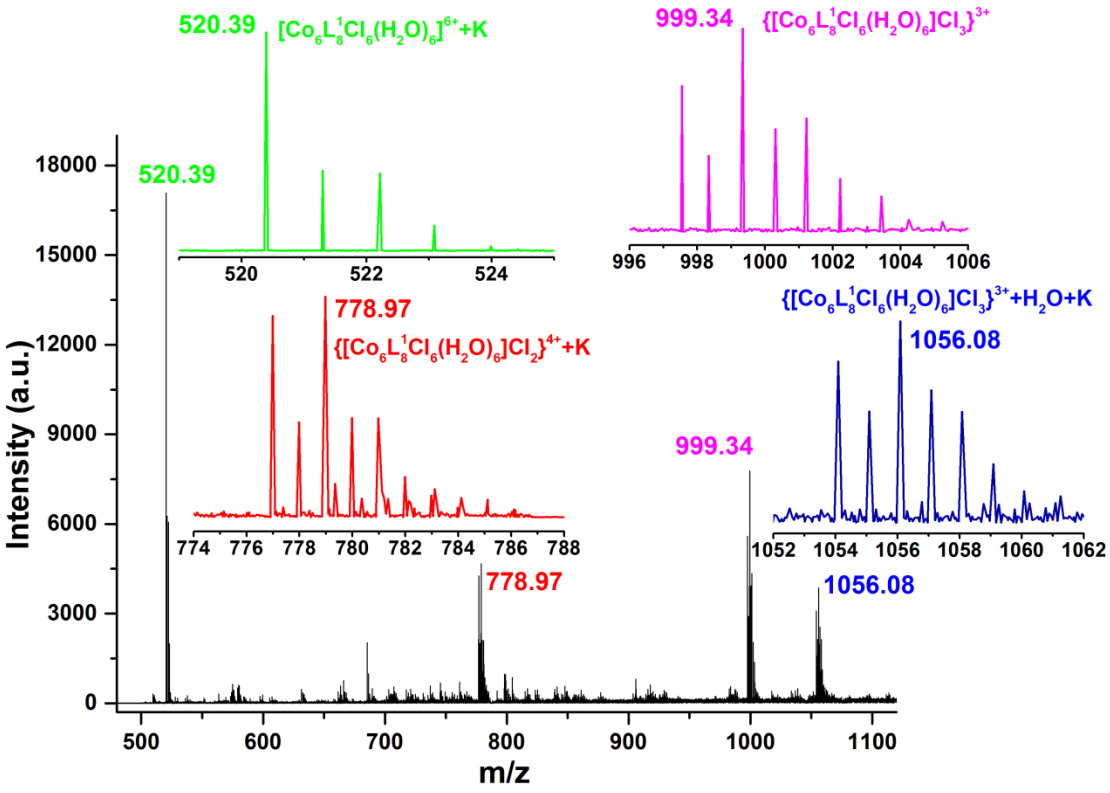

Figure S1. ESI mass spectra of cage **1** in water

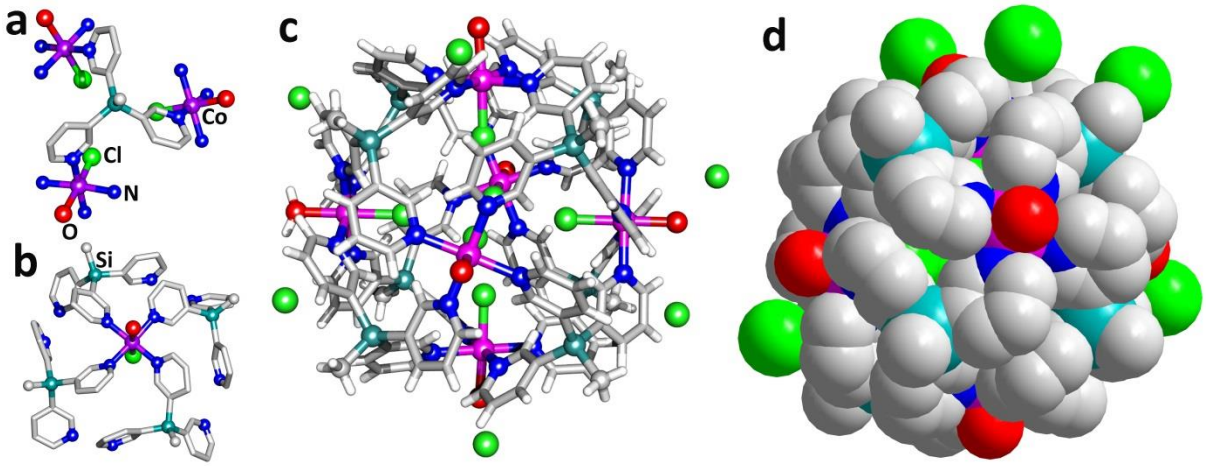

Figure S2. Crystal structure of **1** showing (a) the linkage mode of the ligands, (b) the coordination environment around the Co^{II} ions, (c) view of the octahedral cationic cage along with the location of counter chloride ions and (d) space filling model of cage **1** showing the absence of any cage windows and central cavities

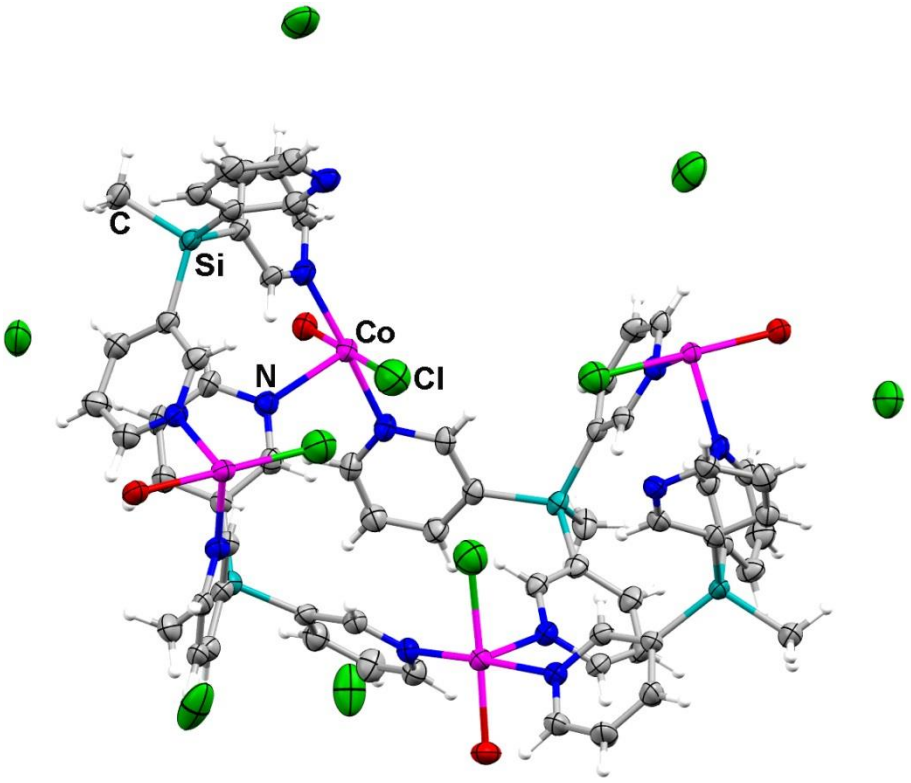

Figure S3: Thermal ellipsoid plot at 50% probability for the asymmetric unit of **1**

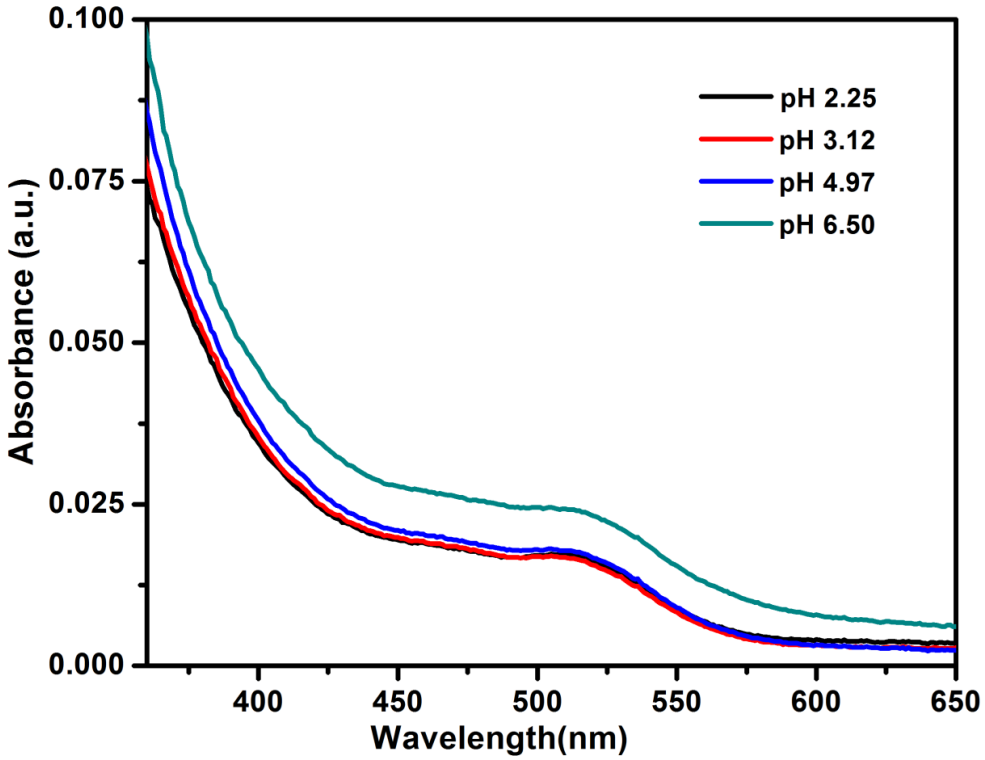

Figure S4. UV-Visible spectra of the 0.2 mM solution of cage **1** in B. R. Buffer at various pH at 25 °C

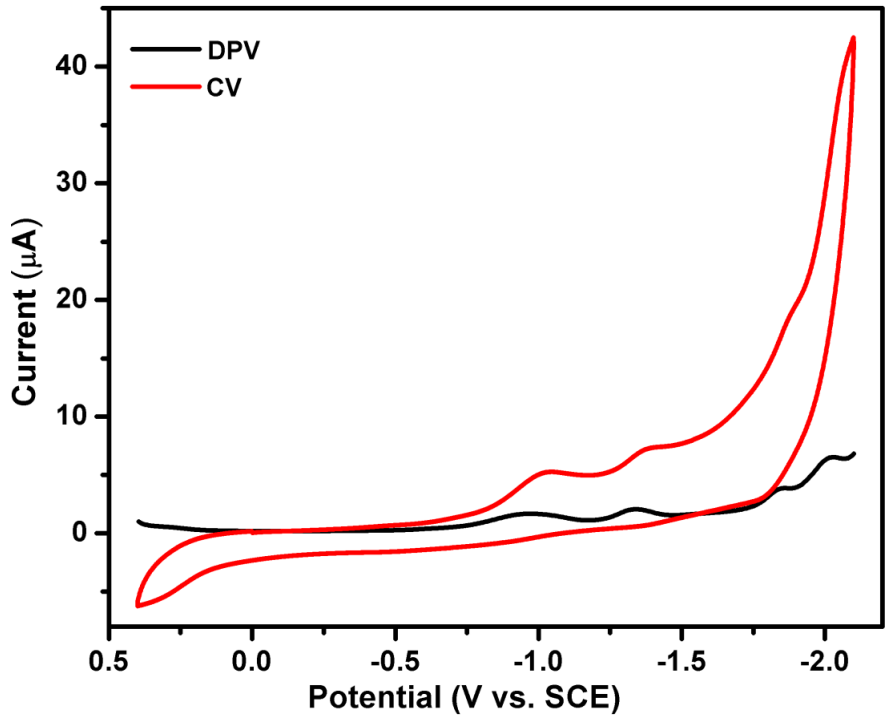

Figure S5. CV (red line) and DPV (black line) of 1 mM of ligand L^1 in acetonitrile at a scan rate 100 mV/s, containing 0.1 M (n-$Bu_4N)PF_6$) as supporting electrolyte and SCE reference electrode, glassy carbon working electrode and Pt wire auxiliary electrode at 25 °C

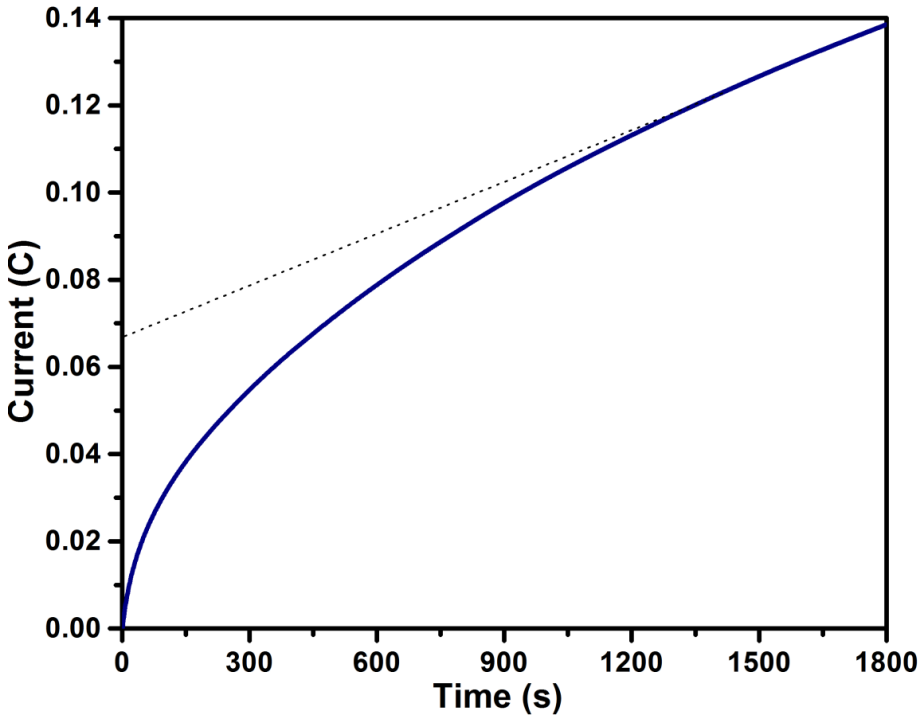

Figure S6: Charge vs time curves for bulk electrolysis of a 5 ml sample of 161 µM (cage **1**), at 0.75 V potential in water. KNO_3 (0.1 M): supporting electrolyte; SCE: reference electrode; glassy carbon: working electrode; Pt wire: uxiliary electrode

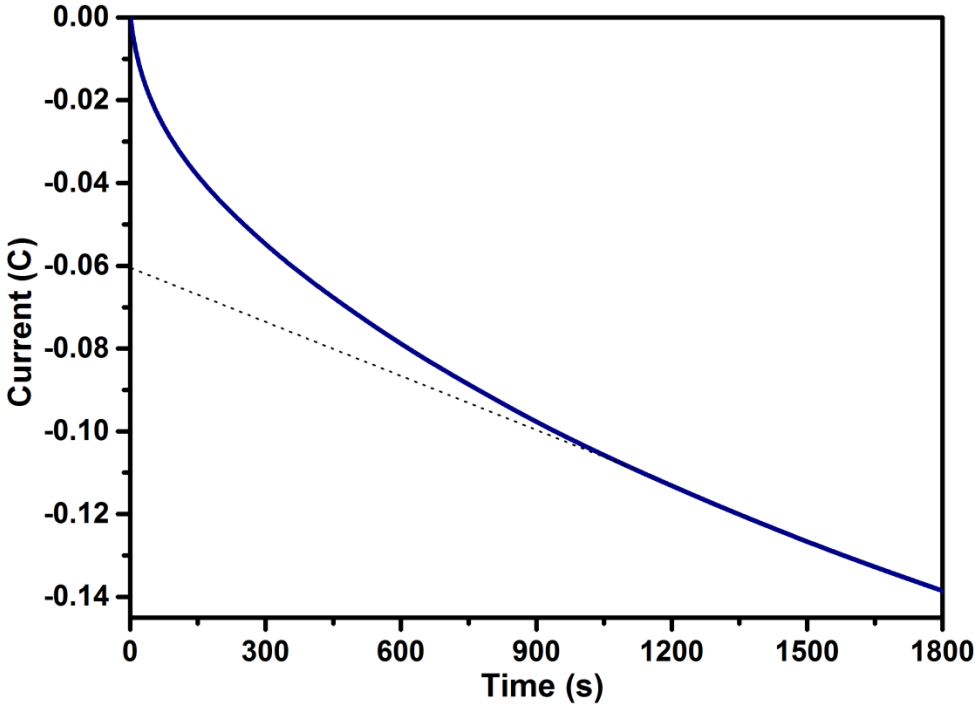

Figure S7: Charge-time curves for bulk electrolysis of a 5 ml sample of 161 µM (cage **1**), at -0.75 V potential in water. KNO_3 (0.1 M): supporting electrolyte; SCE: reference electrode; glassy carbon: working electrode; Pt wire: uxiliary electrode

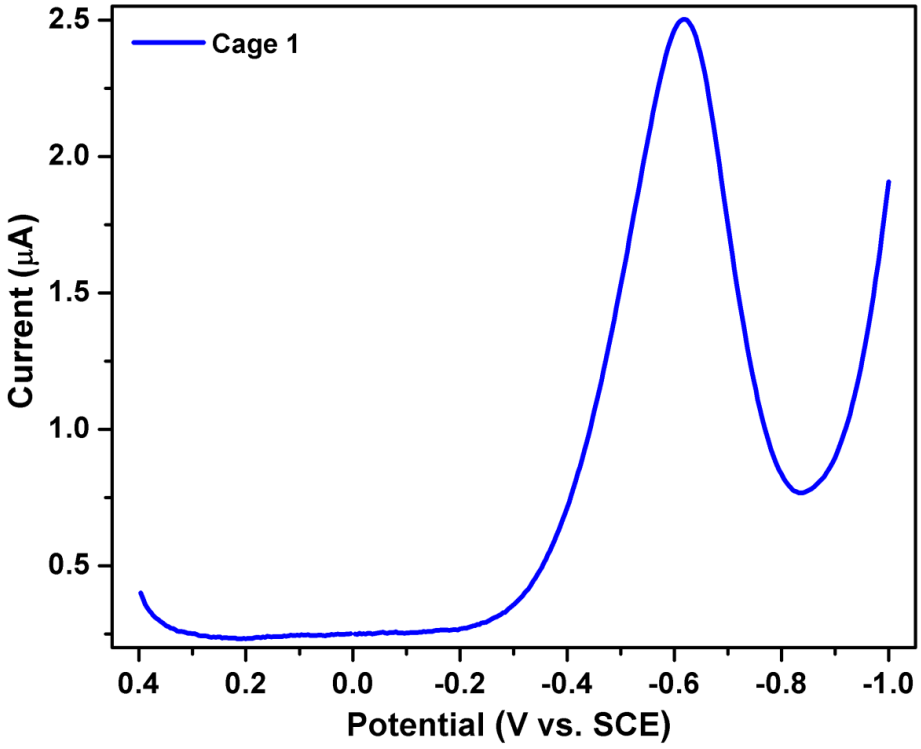

Figure S8. DPV of 1 mM **1** in buffer solution (pH 4) at a scan rate of 100 mV/s at 25 °C, containing 0.1 M (n-$Bu_4N)PF_6$) as supporting electrolyte and SCE as reference electrode, glassy carbon as working electrode and Pt wire as auxiliary electrode

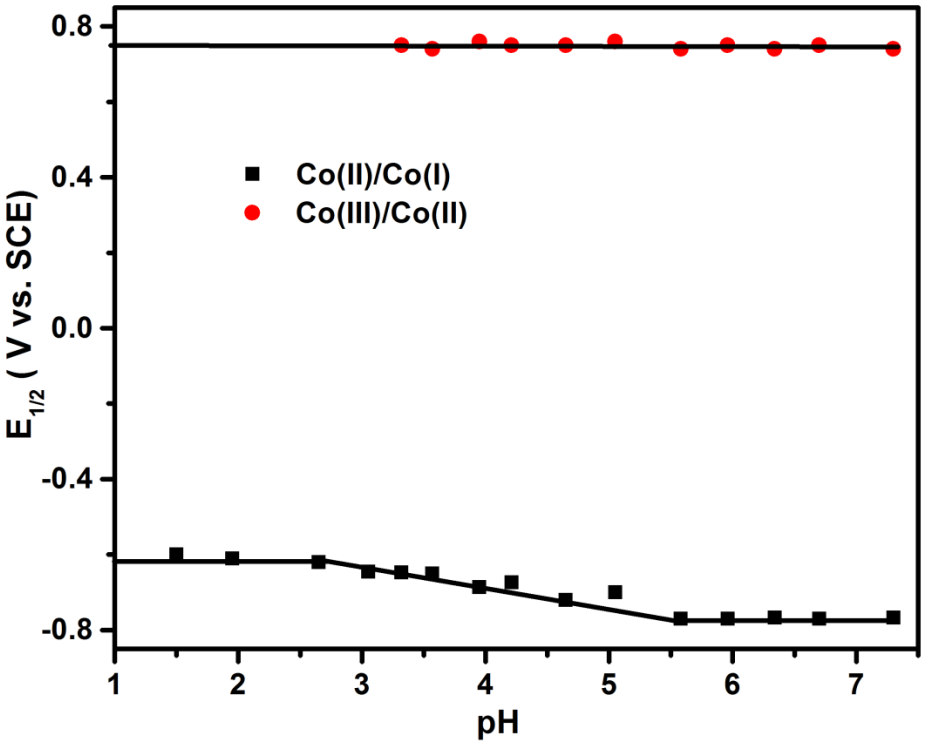

Figure S9. The Pourbiax diagram of 1 mM **1** at 25 ^{0}C in B.R.buffer by using DPV (Differential Pulse Voltammetry)

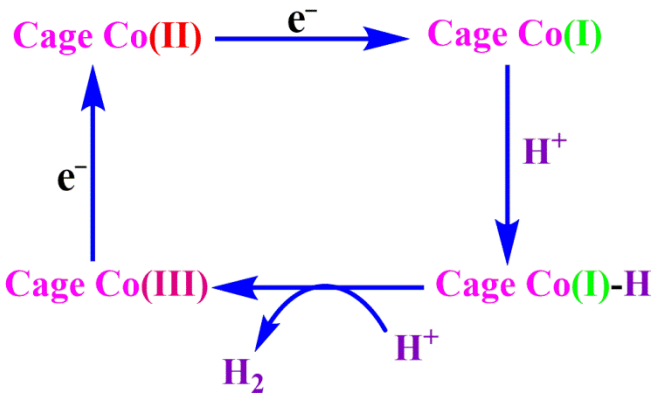

Figure S10: Schematic diagram illustrating the pathway leading to the hydrogen evolution from proton catalysed by the cage 1. The observation of a linear line with a slope (~= -59 mV/pH) in the Pourbiax diagram (Figure S9) indicates the involvement of proton-coupled electron transfer in the catalytic pathway.

Figure S11: Evolution of hydrogen and oxygen bubbles at glassy carbon disk and Pt wire electrodes, respectively

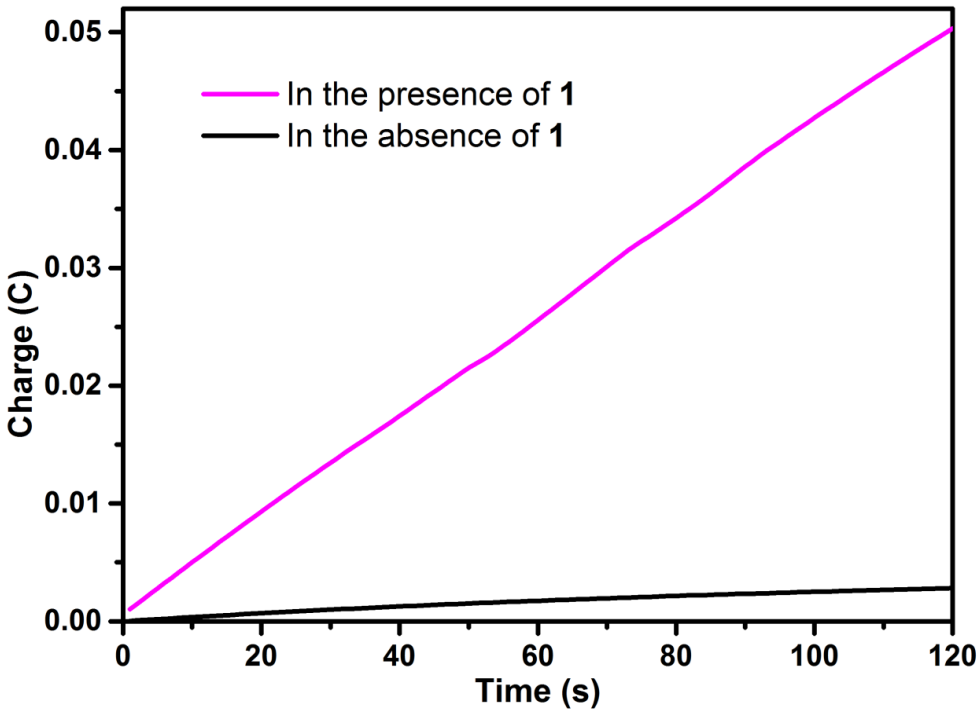

Figure S12: Controlled potential electrolysis at -1.4 V (vs SCE); In the presence (pink line) and absence (black line) of 0.5 µM **1** in 1.0 M aqueous phosphate buffer (pH 7.0); Glassy Carbon as working electrode, Pt wire as counter electrode and SCE as the reference electrode.

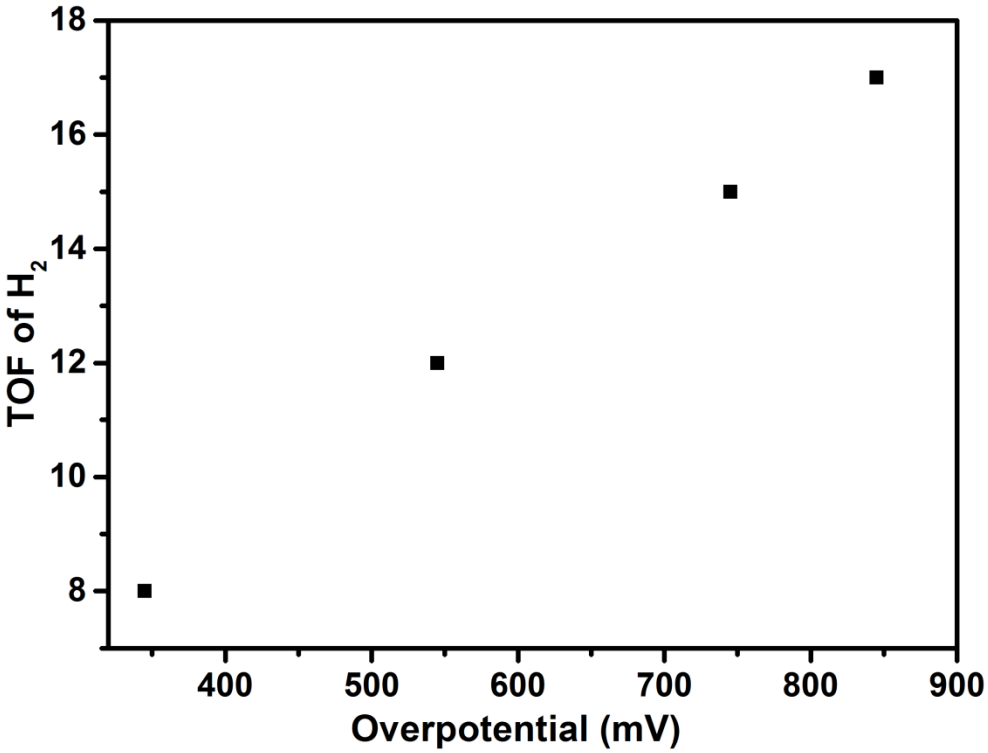

Figure S13: Turnover frequency (mol H_2/mol catalysts/h) versus overpotentials (mV) in 1.0 M phosphate buffer (pH 7.0) for the electrocatalytic hydrogen evolution by **1** (0.5 µM). Overpotential = applied potential – E(pH), where E(pH) = 0.059pH

$$TOF = \Delta C/Fn_1n_2t \text{ ----------> Eqn. S1}$$

Where,

ΔC = Difference between charge build with and without catalyst

F = Faraday's Constant (96480 mol^{-1})

n_1 = Number of electrons involved in the reduction of proton (2)

n_2 = Number of moles of **1**

t = 120 s

Eqn. S1: Calculation of Turnover Frequency (TOF)

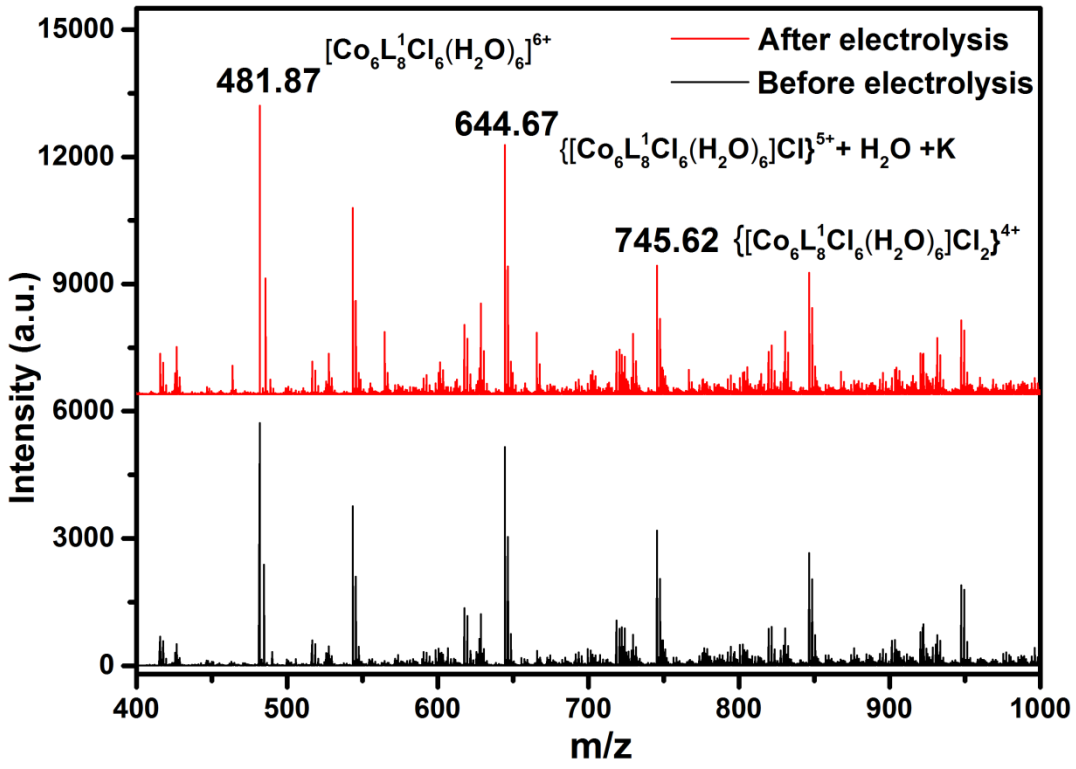

Figure S14: ESI mass spectra of **1** before and after the bulk electrolysis

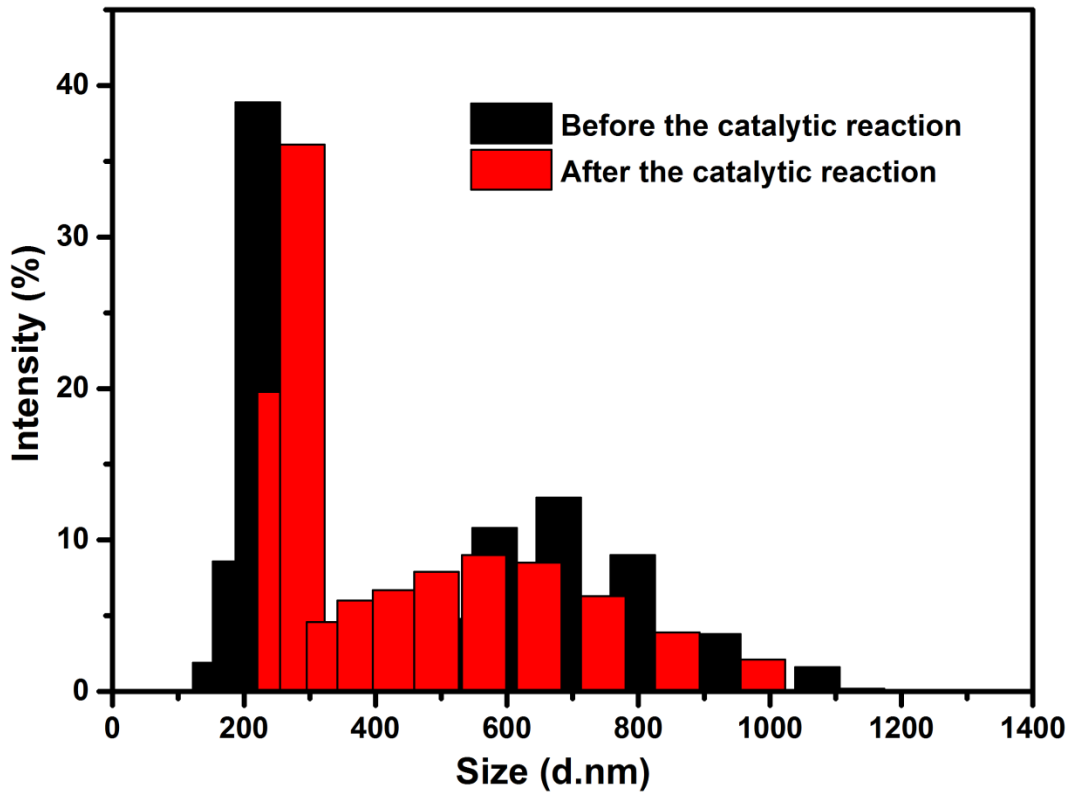

Figure S15: DLS analysis of the photocatalytic system; black bar for before and red bar for after the photocatalytic reaction under inert atmosphere

Table S3: comparative data of photocatalytic activity of Co(II) complexes

Catalysts	[Cat]	conditions	pH	light	TON	Ref.
$[Co(bpyPY_2OH)(CH_3CN)(CF_3SO_3)]^+$	20 µM	H_2A/HA^- (0.3 M), $[Ru(bpy)_3]^{2+}$	4.0	LED 452 nm	950	1
$[Co(bpyPY_2Me)(CH_3CN)(CF_3SO_3)^+$	20 µM	H_2A/HA^- (0.3 M), $[Ru(bpy)_3]^{2+}$	4.5	LED 452 nm	1850	1
$[Co(bpy(PY\text{-}CF_3)_2Me)(CH_3CN)_2]^{2+}$	20 µM	H_2A/HA^- (0.3 M), $[Ru(bpy)_3]^{2+}$	4.5	LED 452 nm	400	1
$[Co(qpy)(OH_2)_2]^{2+}$	20 µM	H_2A/HA^- (0.3 M), $[Ru(bpy)_3]^{2+}$	5.5	LED 452 nm	200	1
$[Co(pr\text{-}bpy_2)(CF_3SO_3)_2]^{2+}$	20 µM	H_2A/HA^- (0.3 M), $[Ru(bpy)_3]^{2+}$	5.0	LED 452 nm	150	1
$[Co(PY_4Me_2H)(CH_3CN)(CF_3SO_3)]^{1+}$	20 µM	H_2A/HA^- (0.3 M), $[Ru(bpy)_3]^{2+}$	5.5	LED 452 nm	250	1
$[Co(PY_4Me_3)(CH_3CN)_2]^{2+}$	20 µM	H_2A/HA^- (0.3 M), $[Ru(bpy)_3]^{2+}$	5.0	LED 452 nm	225	1
$[Co(ppq)Cl_2]$	3 µM	H_2A/HA^- (0.3 M), $[Ru(bpy)_3]^{2+}$	4.0	LED 469 nm	333	2

$[Co(bpy_2PYMe)(CF_3SO_3)]^+$	20 µM	H_2A/HA^- (0.3 M), $[Ru(bpy)_3]^{2+}$	4.0	LED 452 nm	1630	3
$[Co(bpy_2PYMe\text{-}CF_3)(CF_3SO_3)]^+$	20 µM	H_2A/HA^- (0.3 M), $[Ru(bpy)_3]^{2+}$	4.5	LED 452 nm	1390	3
$[Co(CF_3PY_5Me_2)(H_2O)]^{2+}$	50 µM	H_2A/HA^- (0.3 M), $[Ru(bpy)_3]^{2+}$	6.0	LED 452 nm	300	4
$[Co(Py5)Cl]^+$	50 µM	Acetate buffer 1 M H_2A/HA^- (0.1 M), $[Ru(bpy)_3]^{2+}$	4.0	LED 452 nm	187	5
$[Co(ppq)Cl_2]$	10 µM	H_2A/HA^- (0.3 M), $[Ru(bpy)_3]^{2+}$	4.5	LED 469 nm	300	6
$[Co(pbq)Cl_2]$	10 µM	H_2A/HA^- (0.3 M), $[Ru(bpy)_3]^{2+}$	4.5	LED 469 nm	225	6
$[Co(pdpq)Cl(H_2O)]^+$	10 µM	H_2A/HA^- (0.3 M), $[Ru(bpy)_3]^{2+}$	4.5	LED 469 nm	750	6
$[Co(ptpq)Cl_2]$	10 µM	H_2A/HA^- (0.3 M), $[Ru(bpy)_3]^{2+}$	4.5	LED 469 nm	180	6
$[Co(N4py)Cl]^{2+}$	100	H_2A/HA^- (1.1 M),	4.0	LED 452	65	7

	µM	$[Ru(bpy)_3]^{2+}$		nm		
Cage **1**	50 µM	H_2A/HA^- (0.3 M), $[Ru(bpy)_3]^{2+}$	4.0	LED 469 nm	43	Present manuscript

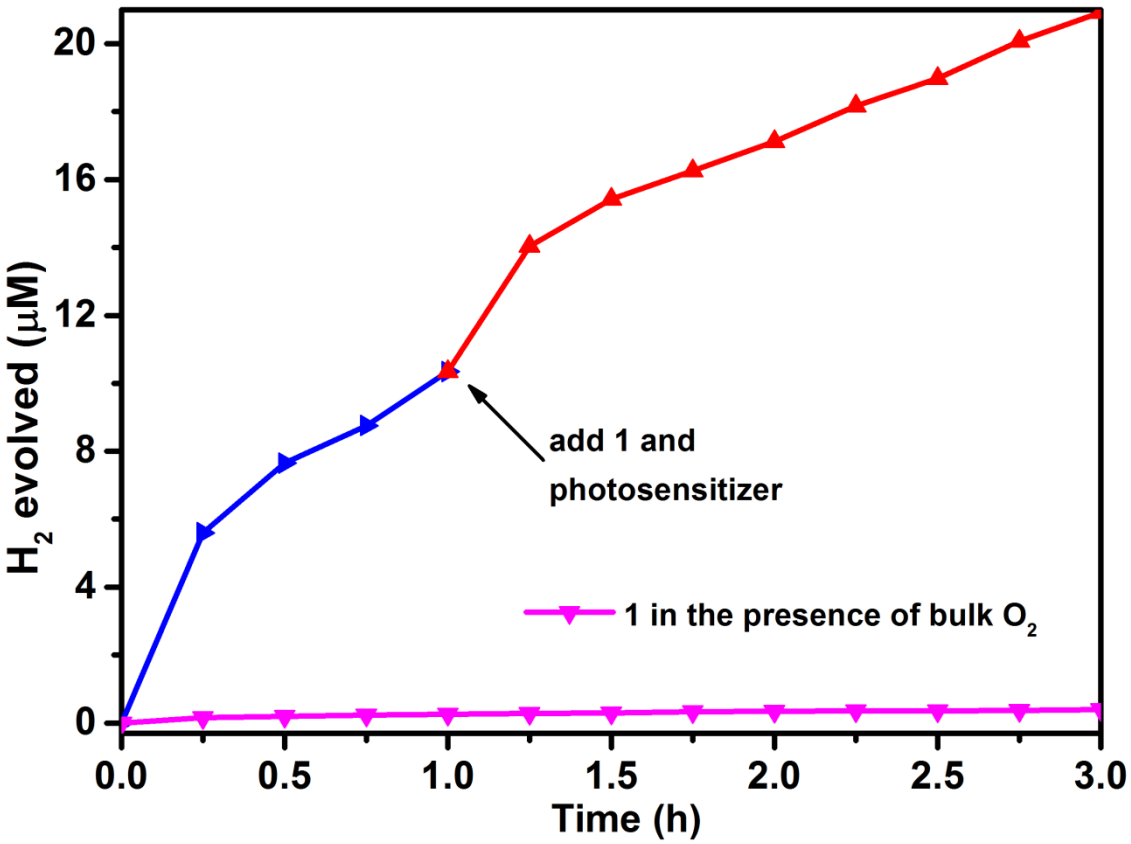

Figure S16: Photocatalytic hydrogen evolution over the time. Conditions: 5 mL 1.0 M acetate buffer at pH 4.0, [ascorbic acid] = 0.3 M, $[Ru(bpy)_3]^{2+}$ = 0.5 mM, [**1**] = 200.0 µM, LED light: 469 nm. The arrow indicates addition of **1** (200.0 µM) and $[Ru(bpy)_3]^{2+}$ (0.5 mM) after hydrogen evolution begins to saturate.

References

1) Khnayzer, R. S.; Thoi, V. S.; Nippe, M.; King, A. E.; Jurss, J. W.; El Roz, K. A.; Long, J. R.; Chang, C. J.; Castellano, F. N. Towards a comprehensive understanding of visible-light photogeneration of hydrogen from water using cobalt (II) polypyridyl catalysts. *Energy. Environ. Sci.*, **2014**, *7*, 1477-1488.

2) Tong, L.; Zong, R.; Thummel, R. P. Visible Light-Driven Hydrogen Evolution from Water Catalyzed by A Molecular Cobalt Complex. *J. Am. Chem. Soc.*, **2014**, *136*, 4881–4884

3) Nippe, M.; Khnayzer, R. S.; Panetier, J. A.; Zee, D. Z.; Olaiya, B. S.; Head-Gordon, M.; Chang, C. J.; Castellano, F. N.; Long, J. R. Catalytic proton reduction with transition metal complexes of the redox-active ligand bpy_2PYMe. *Chem. Sci.*, **2013**, *4*, 3934-3945

4) Sun, Y.; Bigi, J. P.; Piro, N. A.; Tang, M. L.; Long, J. R.; Chang, C. J. Molecular cobalt pentapyridine catalysts for generating hydrogen from water. *J. Am. Chem. Soc.*, **2011**, *133*, 9212-9215.

5) Deponti, E.; Luisa, A.; Natali, M.; Iengo, E.; Scandola, F. Photoinduced hydrogen evolution by a pentapyridine cobalt complex: elucidating some mechanistic aspects. *Dalton Trans.*, **2014**, *43*, 16345-16353.

6) Tong, L.; Kopecky, A.; Zong, R.; Gagnon, K. J.; Ahlquist, M. S.; Thummel, R. P. 2015. Light-Driven Proton Reduction in Aqueous Medium Catalyzed by a Family of Cobalt Complexes with Tetradentate Polypyridine-Type Ligands. *Inorg. chem.*, **2015**, *54*, 7873-7884.

7) Lo, W. K.; Castillo, C. E.; Gueret, R.; Fortage, J.; Rebarz, M.; Sliwa, M.; Thomas, F.; McAdam, C. J.; Jameson, G. B.; McMorran, D. A; Crowley, J. D. Synthesis, characterization, and photocatalytic H_2-evolving activity of a family of $[Co(N_4Py)(X)]^{n+}$ complexes in aqueous solution. *Inorg. Chem.*, **2016**, *55*, 4564-4581.